

Communication

Towards Dry Machining of Titanium-Based Alloys: A New Approach Using an Oxygen-Free Environment

Hans Jürgen Maier ¹, Sebastian Herbst ^{1,*}, Berend Denkena ², Marc-André Dittrich ², Florian Schaper ², Sebastian Worpenberg ², René Gustus ³ and Wolfgang Maus-Friedrichs ³

¹ Institut für Werkstoffkunde (Materials Science), Leibniz Universität Hannover, 30823 Garbsen, Germany; maier@iw.uni-hannover.de

² Institut für Fertigungstechnik und Werkzeugmaschinen (Institute of Production Engineering and Machine Tools), Leibniz Universität Hannover, 30823 Garbsen, Germany; denkena@ifw.uni-hannover.de (B.D.); dittrich@ifw.uni-hannover.de (M.-A.D.); Schaper@ifw.uni-hannover.de (F.S.); worpenberg@ifw.uni-hannover.de (S.W.)

³ Clausthal Centre for Material Technology, Leibnizstraße 9, 38678 Clausthal-Zellerfeld, Germany; rene.gustus@tu-clausthal.de (R.G.); wolfgang.maus-friedrichs@tu-clausthal.de (W.M.-F.)

* Correspondence: herbst@iw.uni-hannover.de; Tel.: +49-511-762-18324

Received: 29 July 2020; Accepted: 21 August 2020; Published: 28 August 2020



Abstract: In the current study, the potential of dry machining of the titanium alloy Ti-6Al-4V with uncoated tungsten carbide solid endmills was explored. It is demonstrated that tribo-oxidation is the dominant wear mechanism, which can be suppressed by milling in an extreme high vacuum adequate (XHV) environment. The latter was realized by using a silane-doped argon atmosphere. In the XHV environment, titanium adhesion on the tool was substantially less pronounced as compared to reference machining experiments conducted in air. This goes hand in hand with lower cutting forces in the XHV environment and corresponding changes in chip formation. The underlying mechanisms and the ramifications with respect to application of this approach to dry machining of other metals are discussed.

Keywords: milling; Ti 64; Ti-6Al-4V; extreme vacuum; tribo-oxidation; built-up edge; microstructure

1. Introduction

Titanium-based alloys are widely used for demanding applications in transportation and energy conversion industries. The most frequently used alloy in this field is Ti-6Al-4V. This material combines excellent corrosion resistance with high strength and low density [1]. Thus, the material is typically employed for aerospace applications, where low weight of the components is a key requirement. In the quest of lightweight design, manufacturing of the aerospace components often involves plenty of milling operations. In fact, the amount of chips removed can make up more than 95% of the initial wrought material [2]. For machining of titanium-based alloys in a cutting speed range between 60 and 120 m min⁻¹, cemented tungsten carbide tools with physical vapor deposition (PVD) coatings are the state of the art and widely used [3]. However, milling of titanium alloys is challenging as the material has low heat conductivity, low elastic modulus, and high chemical reactivity resulting in a strong tendency to build adhesions on the cutting material [4]. Abele and Fröhlich point out that the titanium cutting process is very sensitive to changes in process parameters [5]. Changes have a strong influence on the stability, process safety, and effectiveness of the process. Given the low heat conductivity, the use of lubricants is crucial to cool the cutting tool and avoid degradation of the near-surface layer of the workpiece [6]. Due to the high temperatures in the contact surface, wear is triggered by adhesion and diffusion between tool and workpiece [7]. Hartung et al. suggested that a

reaction layer is formed between the tool and the workpiece material. Its thickness is determined by the rate of diffusion of tool material through this layer and the rate of dissolution of the reaction layer into the workpiece [8]. Nabhani showed a significant diffusion of titanium in cemented carbide and CBN substrates during indentation tests at high temperatures [9]. The diffusion is less pronounced in the contact area between titanium alloy and PCD. Corduan et al. carried out cutting tests with PCD, CBN, and coated carbide in order to understand their behavior, especially concerning chemical reactivity [10]. They found that coatings can protect the cemented carbide tool from diffusion and adhesion; however, high temperatures in the cutting zone result in coating delamination and thermal fatigue. Bushlya et al. investigated the influence of oxygen on tool wear in machining different workpiece materials using an argon atmosphere [11]. The results show that the impact of the atmosphere depends on the tool-workpiece pairing. However, due to a content of oxygen of up to 5 ppmv in technical argon grades, oxidation cannot be completely eliminated.

Today, efficient recycling of the chips is not feasible as these are contaminated by the lubricant. Moreover, oxygen uptake during chip formation degrades the material further. Clearly, dry milling of titanium-based alloys is very attractive both from economic and ecological points of view. The excessive wear resulting from tribo-oxidation is, however, a major roadblock in this context. Thus, the approach used in the present study was to completely eliminate tribo-oxidation by milling in an oxygen-free environment. It has to be noted, however, that technical grades of inert gases such as argon still contain about 5 to 15 ppmv oxygen, which corresponds to a partial pressure of ≈ 1 Pa (10^{-5} bar). According to the equation for the surface impact rate (particle stream density on the surface), the freshly exposed titanium will still experience more than 10^{18} collisions with oxygen molecules per square centimeter and second [12].

Even high-purity inert gas grades (with approx. 0.05 ppmv oxygen) or ultrahigh vacuum are not sufficient to suppress rapid formation of a monolayer of oxygen. Only extreme high vacuum (XHV), with an oxygen partial pressure below 10^{-15} Pa (10^{-20} bar), provides conditions such that oxidation becomes kinetically impossible in the process. In the present study, a SiH_4 -doped argon atmosphere was employed to realize milling of the Ti-6Al-4V samples under XHV-adequate conditions with oxygen partial pressures of $\approx 10^{-19}$ Pa (10^{-24} bar).

2. Materials and Methods

The XHV-adequate atmosphere was realized by doping commercially available argon (≤ 5 ppmv H_2O , ≤ 5 ppmv O_2 , ≤ 10 ppmv N_2) with SiH_4 . Oxygen and water are eliminated according to $\text{SiH}_4(\text{g}) + \text{O}_2(\text{g}) \rightarrow \text{SiO}_2(\text{s}) + 2\text{H}_2(\text{g})$ and $\text{SiH}_4(\text{g}) + 2\text{H}_2\text{O}(\text{g}) \rightarrow \text{SiO}_2(\text{s}) + 4\text{H}_2(\text{g})$ from the atmosphere. As a result, the oxygen partial pressure will drastically decrease when adding only a few ppmv of SiH_4 . The measured oxygen partial pressure in nitrogen as a function of added SiH_4 at 600 °C according to Lützenkirchen-Hecht et al. is depicted in Figure 1 [13]. A similar behavior will result in other inert gases similar to argon and for lower temperatures as employed in the present study. The key difference is that the stoichiometric points, which occur at 6.75 and 13.5 ppmv in Figure 1, will be shifted to lower SiH_4 fractions as the argon used in the present study featured a lower initial oxygen content.

In the present study, specimens of the ($\alpha + \beta$)-titanium alloy Ti-6Al-4V were machined under dry conditions using a milling machine tool Heller PFV 1 (Gebr. Heller Maschinenfabrik GmbH, Nürtingen, Germany). To assess the influence of the environment on the cutting conditions during milling, laboratory air was used as a reference. In order to ensure an oxygen-free atmosphere the test setup shown in Figure 2 was used. The titanium samples were mounted on a baseplate made of aluminum. The baseplate was connected to the working spindle using a flexible plastic housing. The argon, doped with 1.5 vol. % SiH_4 , was introduced into the resulting intermediate space between the baseplate and spindle through a gas inlet on the back of the baseplate. A constant flow of oxygen-free argon ensured that an overpressure inside the plastic housing was set to prevent the surrounding air from reaching the tool. Uncoated tungsten carbide solid endmills, Iscar AL-TEC EC080B20-3C08-63 (Substrate IC08, Iscar Germany GmbH, Ettlingen, Germany) were employed in all experiments. The tool

features a rake angle of $\gamma = 8^\circ$ and a clearance angle of $\alpha = 12^\circ$. All experiments were carried out using a full width of cut $a_e = 8$ mm and a depth of cut $a_p = 1.5$ mm with a cutting speed $v_c = 80$ m/min and a feed per tooth of $f_z = 0.1$ mm. Each experiment consisted of three milling tracks, as shown in Figure 2 on the right side. To measure the cutting forces, a three-component dynamometer of type Kistler 9255B (Kistler Instrumente GmbH, Sindelfingen, Germany) was used. The measured feed force F_f and feed normal force F_{fN} , also shown in Figure 2, were used to contrast differences in the cutting behavior of Ti-6Al-4V during machining in different atmospheres. A scanning frequency of 1000 Hz was used to record these forces. The respective force signal is assigned to the respective force component via the effective direction and averaged on the basis of the time variance of the milling process.

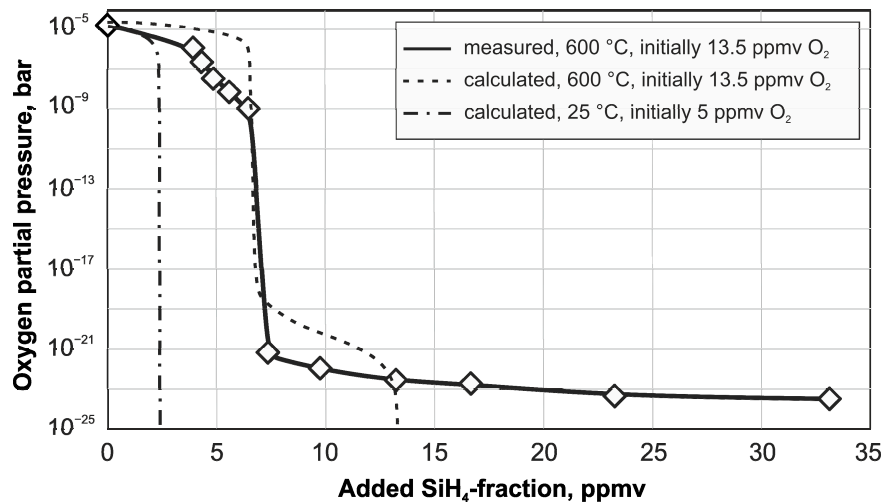


Figure 1. Measured and calculated thermodynamic oxygen activities as a function of added SiH_4 (partly recomputed from [11]).

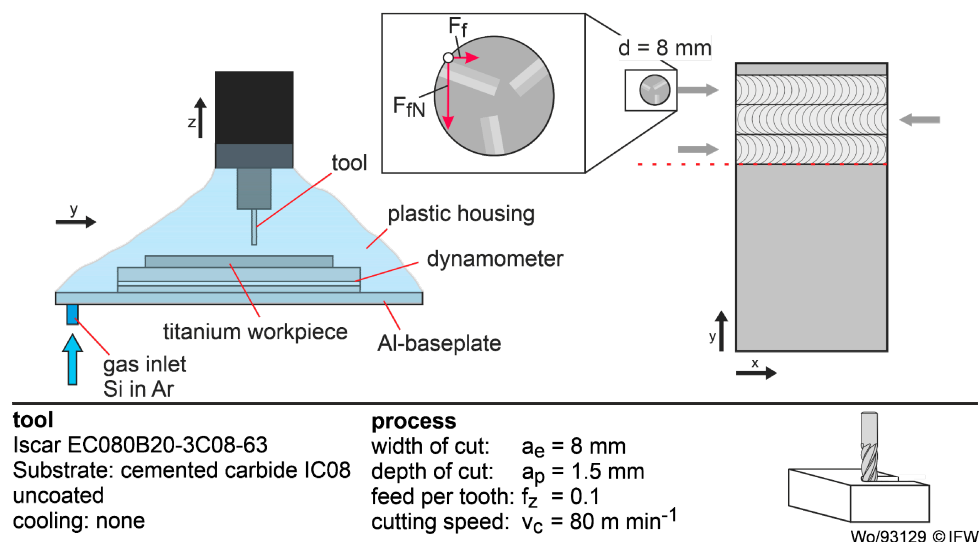


Figure 2. Setup of the dry milling experiments.

To get insight into the microstructure and the chemical composition of the endmills, scanning electron microscopy (SEM) and energy dispersive spectroscopy (EDS) were used. The techniques were supplemented by focused ion beam (FIB) milling, which allows for making well-defined cuts into the sample surface.

For the SEM/EDS measurements and the FIB preparation, a Helios Nanolab 600 (FEI Germany GmbH, Frankfurt, Germany) dual beam system was used. SEM, EDS, and FIB were carried out under high vacuum conditions at a system base pressure of 10^{-4} Pa (10^{-6} mbar). The samples were attached

to a standard SEM sample holder via an adhesive tape. The SEM pictures of the sample surface were recorded at an acceleration voltage of 15 kV and a probe current of 0.69 nA using a through the lens detector (TLD). EDS measurements were carried out at 15 kV and 1.4 nA using a X-Max 80 silicon drift detector (Oxford Instruments, Abingdon, United Kingdom). The FIB cross sectioning was done using Ga ions accelerated to the surface at a voltage of 30 kV, cf. Figure 3. The incisions in the surface were done in at least two steps: First, a rough cut (regular cross section) was performed, which had a stair step structure. Then at least one more milling step, at reduced ion current, was employed to clean the cut and to uncover the microstructure of the material (cleaning cross section).

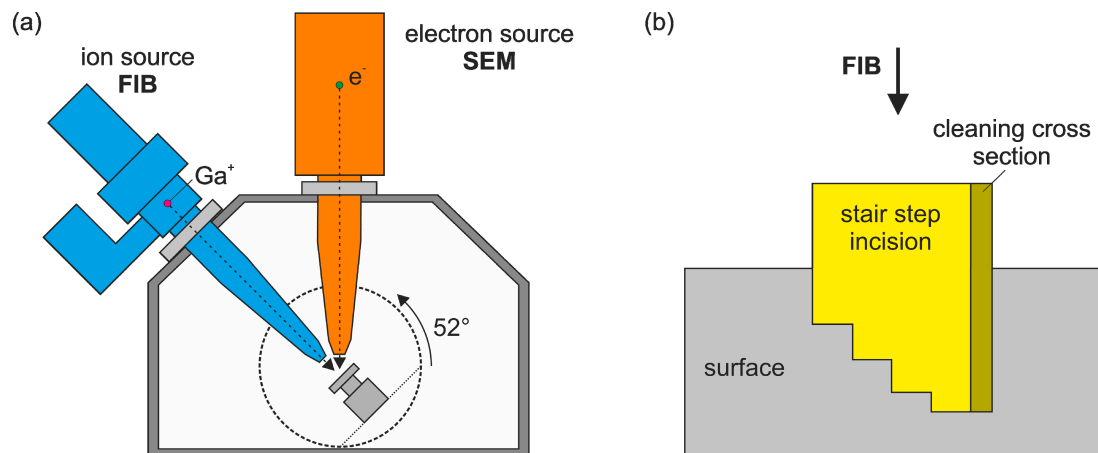


Figure 3. (a) Schematic illustration of the SEM/FIB device along with (b) the approach used for sectioning of the tool surfaces.

3. Results

At first glance, Figure 4 seems to demonstrate that wear of the tool is much more pronounced in the presence of oxygen. A more detailed analysis, however, revealed that the impression in Figure 4 is misleading. As seen in Figure 5, the amount of titanium (green) forming a built-up edge is much less on the tool that was employed in the XHV-adequate environment. Initially, the formation of a built-up edge is not wear. To evaluate the wear, it must first be removed. However, the formation of adhesion on the tools is very different in both cases. The additional carbon (blue) can be attributed to contamination and is not a result of the process.

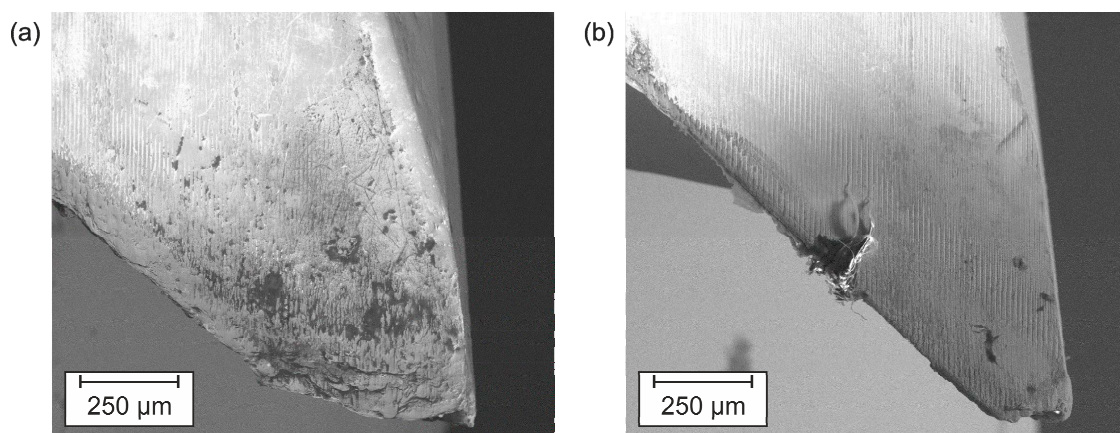


Figure 4. SEM images of the cutting edge after milling in (a) laboratory air and (b) an XHV-adequate environment.

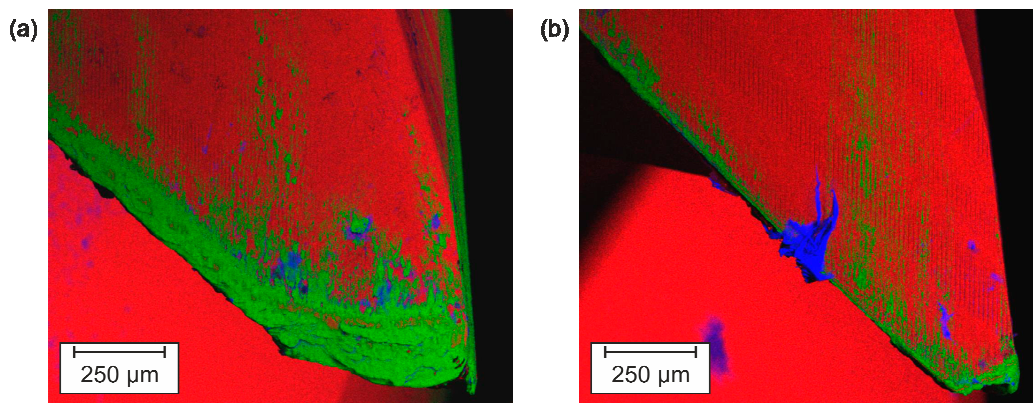


Figure 5. Elemental mappings showing the distribution of titanium on the tool in green after milling in (a) laboratory air and (b) an XHV-adequate environment (red: tungsten; blue: carbon).

Next, the focused ion beam was used to cut a trench into the built-up edge on the tools. From Figure 6, it becomes clear that the initial shape of the cutting edge is still present underneath the titanium layer. Thus, the difference seen in Figure 4 does not result from wear of the tools themselves but is due to substantially different amounts of built-up edge formation upon milling in the two different environments.

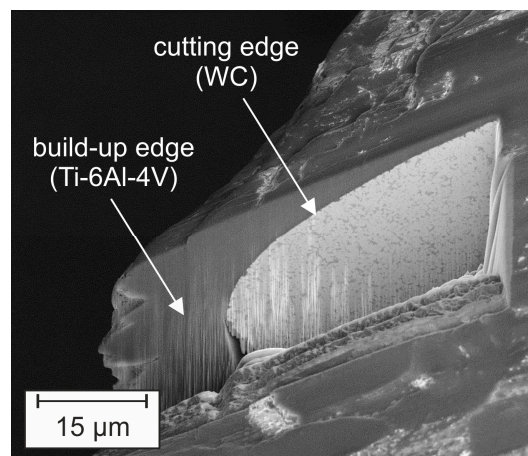


Figure 6. FIB-cut cross section through the cutting edge after machining in laboratory air.

For both conditions, extensive analysis of the local chemical composition along the FIB cuts using EDS was conducted in the SEM. The EDS data reveal that within the experimental scatter, there was no significant difference in the chemical compositions of the built-up edges formed and in the near-surface regions of the tool.

In Figure 7a, process forces during milling of Ti-6Al-4V under different environmental conditions are shown. Therefore, the mean forces $F_{f,mean}$ and $F_{fN,mean}$ were determined. The forces during machining under a silane-containing atmosphere appear significantly lower than under an oxygen-containing atmosphere. Especially the feed forces $F_{f,mean}$, which are about 70% lower for the machining test under an XHV-adequate atmosphere.

To analyze potential differences in chip formation, chips were collected after machining. An analysis of the chip curl radius is presented in Figure 7b. For the evaluation, a sample size of $n = 20$ chips was examined. The resulting chip curl radius is about 16% higher when machining under an XHV-suitable atmosphere, while the achieved roughness of the component surfaces machined in air and in silane-doped argon are at the same level. However, the result for the chip rolling radius is limited by the superposition of scattered surfaces. The collected chips are presented in Figure 8. When machining under an XHV-adequate atmosphere, longer chips are formed. Consequently,

chip thickness is lower, and lower chip compression can be deduced. These observations indicate a significant change in chip formation under oxygen-free conditions, also resulting in a much more energy efficient material deformation. It is also notable that the chip segmentation is much greater and there is a difference in segmentation frequency when machining under an air atmosphere (Figure 8).

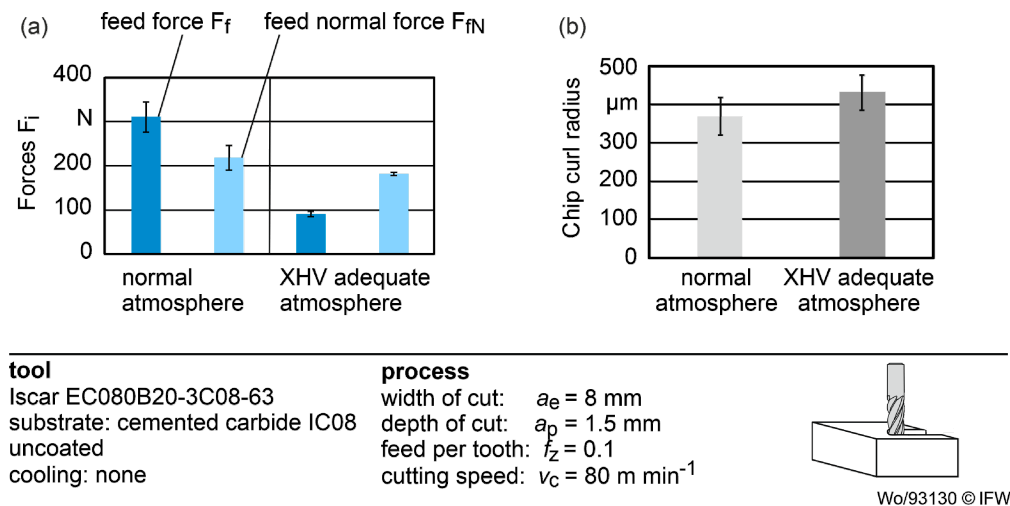


Figure 7. (a) Machining forces and (b) chip curl radius for machining in air and machining under an XHV-adequate atmosphere.

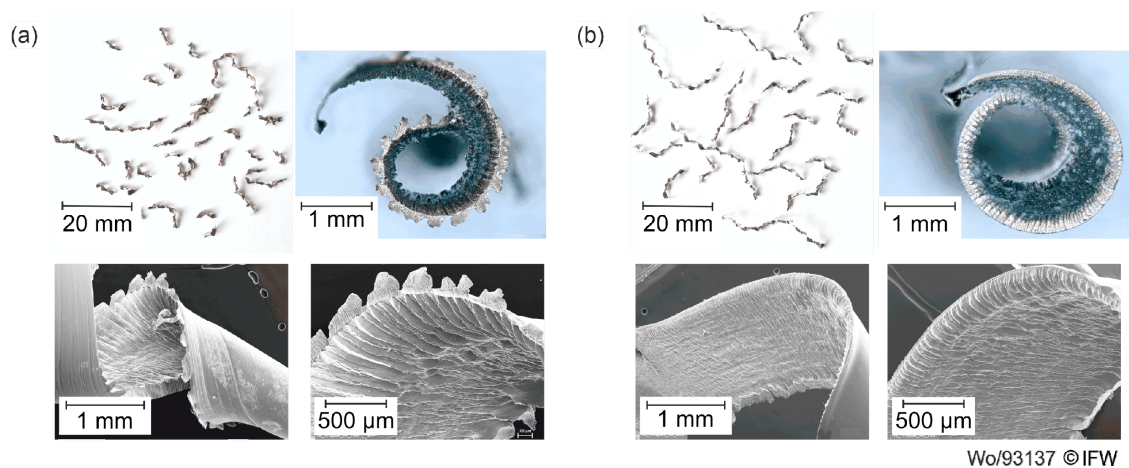


Figure 8. Chips formed during machining (a) under a normal atmosphere and (b) under an XHV-adequate atmosphere.

4. Discussion

The SEM analysis of the tools clearly reveals that adhesions on rake face and flank face are substantially less pronounced upon milling in an XHV-adequate environment (Figure 5). This can be explained as follows. Adhesion on the rake and free face of the tool lead to changes in the effective chip and clearance angle and to changes in the cutting edge microgeometry. From Bergmann, it is well known that the microgeometry of the cutting edge has a significant influence on the machining process [14]. With increasing cutting edge rounding, there is an increase in cutting and feed force, whereby the feed force reacts more sensitively to changes in the cutting edge rounding. For this reason, machining with small cutting edge rounding is recommended for titanium machining. Bergmann reports significant increases especially in the feed force during machining with large cutting edge rounding. Wyen and Wegener have also made these observations [15]. Strong adhesions on the tool lead to an increase in the effective cutting edge radius which, in turn, results in an increase of the minimum chip thickness and, thus, the proportion of material that is displaced under the cutting

edge. The elastic springback increases the contact with the flank face and, hence, the mechanical load in the flank face. This results in higher feed forces. During machining under an XHV-adequate atmosphere, the formation of strong adhesions on the rake face and the flank face of the tool is eliminated. The formation of adhesion in the tool also essentially influences the friction between the chip and the rake face of the tool. Zhang et al. observed lower friction during machining of Inconel 718 with decreasing adhesion to the tool, which also lead to a decrease in process forces to a certain extent [16]. As demonstrated in the presented machining under an XHV-adequate atmosphere, the absence of oxygen resulted in a decrease in titanium adhesion. The formation of adhesion changes the tool geometry and, thus, the frictional behavior between tool and workpiece. In the present case, the workpiece material was identical in each experiment. Therefore, the observed differences can be explained by different friction conditions between chip and tool. At this point, further investigations are necessary in order to determine the formation of boundary layers on the machined material and of adhesions on the tool during machining under an XHV-adequate atmosphere.

A substantial difference in chip formation was also noticeable when machining under different atmospheric conditions. There was a slight increase in chip curl radius and a decrease in chip segmentation when machining under an XHV-adequate atmosphere. According to Grove et al., the chip curl radius is influenced by the thermal properties of the workpiece material [17]. Arrazola et al. showed, by numerical simulation, that the chip curl radius significantly depends on the frictional behavior between tool and workpiece [18]. According to Cook, segmentation occurs with increasing temperature in the deformation zone of the chip [19]. Wu et al. have examined the influence of rake angle on the chip formation when machining TC21 [20]. They found that a larger tool rake angle can decrease the extent of serrated chips and the segmentation frequency. The lower segmentation of the chips during machining in air can be attributed to the different contact conditions caused by the adhesions on the free face and the rake face of the tool.

As demonstrated in the current study, oxygen-free milling is a viable approach to minimize built-up edge formation when machining a titanium-based alloy. The formation of adhesion is still a key issue in machining for many other materials as well. The formation mechanisms could, however, be substantially different. For instance, recent simulation results by Childs et al. have demonstrated that blue-brittle effects induced by thermal hardening and friction resistance to slip seem to be the governing factors that control built-up edge formation in machining of steel [21]. In such a system, tribo-oxidation might be less important. It is still unclear in which systems oxygen-free machining can really be exploited, and additional work is underway to address this issue.

5. Conclusions

Dry milling of a Ti-6Al-V4 alloy with a commercial tungsten carbide tool was studied in both air and an extreme high vacuum (XHV)-adequate (oxygen-free) environment. The results of this study can be summarized as follows:

1. Tribo-oxidation, which is the dominant wear mechanism upon conventional dry milling in this system, is suppressed upon milling in an oxygen-free environment. Thus, this novel approach renders dry milling viable for advanced machining of Ti-based alloys with cemented carbide tools.
2. Cutting forces are lower in the oxygen-free environment and the formation of adhesion is reduced.
3. Chip formation changes in the respective environments due to changes in tool geometry and friction conditions.
4. Oxygen partial pressures corresponding to XHV environments can be easily realized by milling in a SiH₄-doped argon atmosphere.

Author Contributions: Conceptualization, H.J.M. and W.M.-F.; methodology, S.W. and R.G.; investigation, M.-A.D. and R.G.; resources, H.J.M., B.D. and W.M.-F.; writing—original draft preparation, S.H.; writing—review and editing, M.-A.D., F.S., S.W. and R.G.; visualization, S.H., F.S., S.W. and R.G.; supervision, H.J.M., B.D. and W.M.-F.; project administration, S.H.; funding acquisition, H.J.M., B.D. and W.M.-F. All authors have read and agreed to the published version of the manuscript.

Funding: Parts of this work were funded by the Deutsche Forschungsgemeinschaft (DFG, German Research Foundation)—Project-ID 394563137-SFB 1368.

Acknowledgments: The authors thank Ulrich Holländer for determining the thermodynamic activities in the SiH₄-containing atmospheres.

Conflicts of Interest: The authors declare no conflict of interest.

References

1. Veiga, C.; Davim, J.P.; Laureiro, A.J.R. Properties and applications of titanium alloys: A brief review. *Rev. Adv. Mater. Sci.* **2012**, *32*, 133–148.
2. Denkena, B.; Dittrich, M.-A.; Jacob, S. Energy Efficiency in Machining of Aircraft Components. *Proc. CIRP* **2016**, *48*, 479–482. [[CrossRef](#)]
3. Veiga, C.; Davim, J.P.; Loureiro, A.J.R. Review on machinability of titanium alloys: The process perspective. *Rev. Adv. Mater. Sci.* **2013**, *34*, 148–164.
4. Davim, J.P. *Machining of Titanium Alloys*, 1st ed.; Springer: Heidelberg, Germany, 2014.
5. Abele, E.; Fröhlich, B. High speed milling of titanium alloys. *Adv. Prod. Eng. Manag.* **2008**, *3*, 131–140.
6. Pramanik, A. Problems and solutions in machining of titanium alloys. *Int. J. Adv. Manuf. Technol.* **2014**, *70*, 919–928. [[CrossRef](#)]
7. Venugopal, K.A.; Paul, S.; Chattopadhyay, A.B. Growth of tool wear in turning of Ti-6Al-4V alloy under cryogenic cooling. *Wear* **2007**, *262*, 1071–1078. [[CrossRef](#)]
8. Hartung, P.D.; Kramer, B.M.; von Turkovich, B.F. Tool Wear in Titanium Machining. *CIRP Ann.* **1982**, *31*, 75–80. [[CrossRef](#)]
9. Nabhani, F. Wear mechanisms of ultra-hard cutting tools materials. *J. Mater. Process. Technol.* **2001**, *115*, 402–412. [[CrossRef](#)]
10. Corduan, N.; Himbart, T.; Polachon, G.; Dessoly, M.; Lambertin, M.; Vigneau, J.; Payoux, B. Wear mechanisms of new tool materials for Ti-6Al-4V High performance machining. *CIRP Ann.* **2003**, *52*, 73–76. [[CrossRef](#)]
11. Bushlya, V.; Lenrick, F.; Ståhl, J.-E.; M'Saoubi, R. Influence of oxygen on the tool wear in machining. *CIRP Ann.* **2018**, *67*, 79–82. [[CrossRef](#)]
12. Wutz, M.; Adam, H.; Walcher, W.; Jousten, K. *Handbuch Vakuumtechnik*, 12th ed.; Springer Vieweg: Wiesbaden, Germany, 2018.
13. Lützenkirchen-Hecht, D.; Wulff, D.; Wagner, R.; Frahm, R.; Holländer, U.; Maier, H.J. Thermal anti-oxidation treatment of CrNi-steels as studied by EXAFS in reflection mode: The influence of monosilane additions in the gas atmosphere of a continuous annealing furnace. *J. Mater. Sci.* **2014**, *49*, 5454–5461. [[CrossRef](#)]
14. Bergmann, B. Grundlagen zur Auslegung von Schneidkantenverrundungen. Ph.D. Thesis, Leibniz Universität, Hannover, Germany, 2017.
15. Wyen, C.-F.; Wegener, K. Influence of cutting edge radius on cutting forces in machining titanium. *CIRP Ann.* **2010**, *59*, 93–96. [[CrossRef](#)]
16. Zhang, S.; Li, J.F.; Wang, Y.W. Tool life and cutting forces in end milling Inconel 718 under dry and minimum quantity cooling lubrication cutting conditions. *J. Clean. Prod.* **2012**, *32*, 81–87. [[CrossRef](#)]
17. Grove, T.; Denkena, B.; Maiß, O.; Krödel, A.; Schwab, H.; Kühn, U. Cutting mechanism and surface integrity in milling of Ti-5553 processed by selective laser melting. *J. Mech. Sci. Technol.* **2018**, *32*, 4883–4892. [[CrossRef](#)]
18. Arrazola, P.J.; Özel, T.; Umbrello, D.; Davies, M.; Jawahir, I.S. Recent advances in modelling of metal machining processes. *CIRP Ann.* **2013**, *62*, 695–718. [[CrossRef](#)]
19. Cook, N.H. Chip formation in machining titanium. In Proceedings of the Symposium on Machine Grind, Watertown Arsenal, MA, USA, 31 March 1953; pp. 1–7.
20. Wu, H.M.; To, S. Serrated chip formation and their adiabatic analysis by using the constitutive model of titanium alloy in high speed cutting. *J. Alloys Compd.* **2015**, *629*, 368–373. [[CrossRef](#)]
21. Childs, T.H.C. Towards simulating built-up-edge formation in the machining of steel. *CIRP J. Manuf. Sci. Technol.* **2011**, *4*, 57–70. [[CrossRef](#)]

